The optimized power flow control system for the photovoltaic DC microgrid

Elvin Yusubov[1*], *Lala* Bekirova[2]

[1]Azerbaijan State Oil and Industry University, Instrumentation Engineering Department, AZ1010, Baku, Azerbaijan
[2]Azerbaijan State Oil and Industry University, Instrumentation Engineering Department, AZ1010, Baku, Azerbaijan

Abstract. The power flow control systems play a significant role in DC microgrids with photovoltaic inputs to supply the load with continuous power. The output power of the photovoltaic modules could experience a decline due to fluctuations in solar irradiation and temperature, which necessitates the use of batteries and the utility grid to reduce the negative effects of undesirable variations. However, an efficient control strategy is necessary to ensure an uninterrupted energy supply to the load units. This paper proposes an improved control of energy flow based on a State-of-Charge battery power estimation technique using the Coulomb counting method. By accurately estimating the available power from the batteries using the State-of-Charge technique, the microgrid is able to determine to assess if it requires to switch to the grid when the power output from photovoltaic modules is insufficient to meet the load demand. The proposed method also eliminates the need for DC bus voltage level-based approaches to charge or discharge the batteries with the advantages of the significant reduction in DC bus voltage variations. The simulation results of the proposed approach show that it provides satisfactory control performance to meet the load demand.

1 Introduction

DC microgrid energy storage and control systems have become increasingly important as a means of providing reliable and sustainable power supply in various applications, such as in remote areas, electric vehicles, and smart buildings. The DC microgrid comprises a network of interconnected power sources, storage devices, and loads that operate at low DC voltages [1, 2]. The simple structure of the DC microgrid is shown in Figure 1. The microgrid can operate independently or can be connected to the main power grid [3]. Energy storage and control systems play a crucial role in DC microgrids by ensuring the continuous power supply to the loads, regardless of changes in the power supply or demand [4-7]. The primary function of energy storage systems is to store excess power when it is available and release it when there is a shortage. Control systems, on the other hand, manage and coordinate the operation of the different components in the microgrid to ensure optimal performance and efficiency.

* Corresponding author: elvinyusifov05@gmail.com

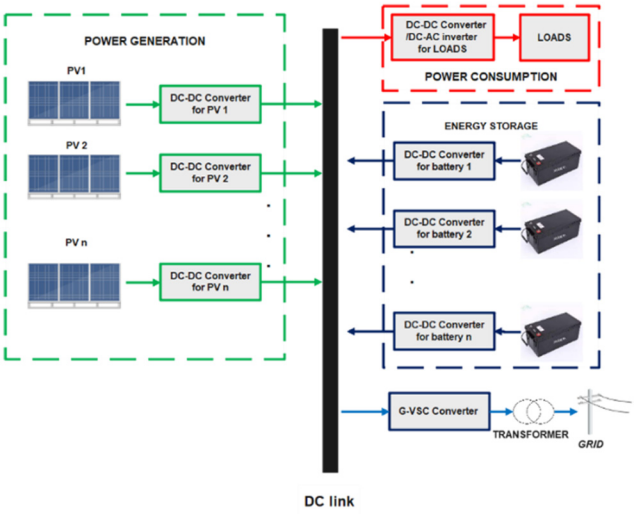

Fig. 1. Simple DC microgrid model.

The integration of renewable energy sources, such as solar PV and wind power, in DC microgrids has provided an opportunity to reduce carbon emissions and promote sustainable energy use. However, the variable nature of these energy sources presents a challenge in maintaining a stable power supply to the load [8, 9]. To mitigate this challenge, energy flow control systems are employed to balance the power supply and demand in the microgrid.

Several strategies are developed to achieve efficient power delivery to the load. In recent times, numerous authors have employed the Kalman filter (KF), a robust algorithm, for estimating the State of Charge (SoC). However, this approach faces a significant limitation in that a suitable battery model is required for the KF to operate effectively [10]. The energy management of the DC microgrid can be considered either in autonomous or grid-connected modes. Although the autonomous mode is useful where the grid power is not available, DC microgrids with utility grids can perform efficiently to compensate for the possible power fluctuations in PV modules and batteries. However, many existing grid-connected DC microgrids do not have an efficient switching strategy to the grid, since the grid power usage must be minimized to minimize energy cost [11, 12]. DC bus signalling methods are one of the prominent methods employed in battery management systems to control the charging and discharging of the battery units. In the DC bus signalling method, the DC bus voltage determines the charging or discharging of the battery units [13, 14]. Noise and interference susceptibility, low interoperability and compatibility, limited transmission distance and low-speed communication are the primary disadvantages of this method.

The primary aim of the paper is to develop an efficient power flow control system for DC microgrids to reduce the shortcomings of the above-mentioned methods.

2 System modelling

To create an efficient energy control system, the internal power flow structure of the DC microgrid must be understood.

2.1 PV modules to DC bus connection

To extract maximum power from the PV modules, MPPT trackers are employed. MPPT controllers are electronic devices used to optimize the power output of photovoltaic solar panels. The maximum power point (MPP) is the point at which a solar panel operates at its maximum power output. MPPT controllers track the MPP of the solar panel and adjust the voltage and current to maintain it at this point. It increases the efficiency of the solar panel, enabling it to produce more power. MPPT controllers are commonly used in both off-grid and grid-connected solar systems to charge batteries, power electrical loads, and feed excess power back into the grid. For higher efficiency, the Moth-Flame optimization-based MPPT controller is employed in the modelling of the DC microgrid [15].

2.2 Battery pack to DC bus connection

The process of connecting a battery pack to a DC bus involves establishing both electrical and physical connections between these two components. A battery pack consists of multiple battery cells linked together to provide a specific voltage and capacity, while the DC bus serves as a distribution system that connects various components within a system. To ensure a safe and efficient connection between the battery pack and the DC bus, a power electronics interface is utilized. This interface employs bidirectional converters, allowing energy to flow in two directions: from the battery pack to the DC bus and vice versa. In the modelling of DC microgrids, the bidirectional SEPIC-ZETA converter is commonly used as it enables the charging or discharging of the batteries without requiring a change in the DC bus voltage.

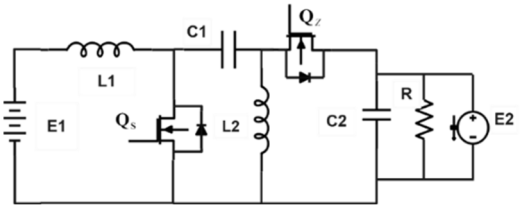

Fig. 2. Bidirectional SEPIC-ZETA converter.

The bidirectional SEPIC-ZETA converter, depicted in Figure 2, contains the following components:

• V_{E1} and V_{E2} are the battery voltage and DC bus voltage, respectively.

•C_1, C_2 are the capacitors,

•L_1, L_2 are the inductors,

• Q_s and Q_z are transistors,

• R is the load resistance.

The bi-directional SEPIC-ZETA DC-DC converters are equipped with two switching transistors that allow the power to flow in two directions. These converters can be used for battery charging and discharging modes in the DC-DC converter mode.

During battery discharge mode (mode 1), the bi-directional SEPIC-ZETA converter is utilized to transfer the stored energy from the batteries to the DC bus. In this mode, the converters act as a SEPIC converter by switching Q_z transistor off, and activating Q_s transistor. The average dynamic model of the SEPIC converter is constructed with the following equations:

$$L_1 \frac{di_{L1}}{dt} = V_{E1} - (1-D)(V_{C1} + V_{C2}) ; \quad (1)$$

$$L_2 \frac{di_{L2}}{dt} = DV_{C1} - (1-D)V_{C2} ; \quad (2)$$

$$C_1 \frac{dV_{C1}}{dt} = (1-D)i_{L1} - Di_{L2} ; \quad (3)$$

$$C_2 \frac{dV_{C2}}{dt} = (1-D)(i_{L1} + i_{L2}) - \frac{V_{C2}}{R}, \quad (4)$$

where i_{L1} is the current through the inductor L_1, i_{L2} is the current through the inductor L_2, V_{C1} is the voltage across the capacitor C_1, V_{C2} is the voltage across the capacitor C_2, V_{E1} is the battery voltage, R is the load resistance, D-duty-cycle corresponding to the on the state of the transistor, *1-D* is the duty cycle corresponding to the off state of the transistor.

During battery charging mode, the bi-directional ZETA converter is activated and charges the batteries using the DC bus power. In this mode, the converter operates in ZETA mode, and transistor Q_z is activated, while transistor Q_s is closed. The average dynamic model of the ZETA converter is constructed with the following equations:

$$\frac{di_{L2}}{dt} = D\frac{V_{C2}}{L_2} + (1\text{-D})\frac{V_{C1}}{L_2}; \quad (5)$$

$$\frac{di_{L1}}{dt} = D\left(\frac{V_{C2}}{L_1} - \frac{V_{C1}}{L_1}\right) - \frac{V_{E1}}{L_1}; \quad (6)$$

$$\frac{dV_{C1}}{dt} = D\frac{i_{L1}}{C_1} - (1\text{-D})\frac{i_{L2}}{C_1}. \quad (7)$$

2.3 VSC Connection

The G-VSC (Grid-Connected Voltage Source Converter) is responsible for managing power transfer between the main grid and the DC microgrid. Its primary function is to regulate the voltage of the DC link to the desired level. When there is a power shortage in the network, the G-VSC controller generates signals to import power from the main grid. Conversely, in situations of excess power, the G-VSC exports power to the utility while ensuring that the DC link voltage remains stable. However, the maximum current capacity of the G-VSC is limited by the converter controls at its nominal value. This limitation restricts the G-VSC's ability to effectively regulate the DC bus voltage in the grid-connected mode of operation.

2.4 Battery SoC estimation

The State-of-Charge (SoC) of a battery refers to the current level of its capacity, represented as a percentage of its maximum capacity. It is a crucial metric used to measure the amount of energy stored in the battery relative to its full capacity. SoC plays a vital role in battery management systems as it helps to determine the remaining energy available and the rate at which the battery can be charged or discharged. The general mathematical formula for SoC is the following:

$$SoC(t) = \frac{Q_{actual}}{Q_{rated}}\ 100\%, \quad (8)$$

where Q_{rated} and Q_{actual} are the capacity of the battery packs.

The Coulomb calculation method is based on the available battery capacity, the number of charges entering and leaving the battery [11].

$$SoC(t) = SoC(t_0) - \frac{1}{Q_{rated}} \int_{t_0}^{t_0+\tau} \eta I_b(t) dt, \quad (9)$$

where,

$SoC(t_0)$ is the initial SoC,

I_b- is battery current,

η_b efficiency of the battery (between 0 and 1).

The precision of the measurement method provided relies heavily on accurately determining the battery's current and initial state of charge (SoC). By obtaining the initial charge value, it becomes feasible to calculate the battery's SoC by integrating the charge and discharge currents over a specific timeframe. However, it's important to note that the amount of charge discharged during charging and discharging is consistently lower than the accumulated charge in the battery. This implies the presence of energy losses during the charging and discharging process, which are characterized by the efficiency coefficient.

The battery operates in three different modes: charging, discharging, and when there is no circuit connected, known as the open circuit mode.

In the charging mode, the battery's voltage and current are provided through constant sources of current and voltage, respectively. By maintaining a constant charging current, the battery's voltage gradually rises and approaches the specified threshold. When charging the battery in voltage mode, the charging current initially decreases rapidly and then at a slower rate. Eventually, when the battery reaches full charge, the current value becomes 0.

In the discharging mode, the voltage at the battery terminals gradually decreases over time. A higher current load leads to a faster decline in terminal voltage, resulting in a reduced duty cycle. By examining the relationship between the state of charge (SoC) and the discharge voltage at various current values, we can determine the initial SoC during the discharge period.

In open circuit mode, the battery is disconnected from the load circuit. The open circuit voltage can be used to determine SoC. To find the current from (9).

$$I_b(t) = -\frac{Q_{rated.}}{\eta} \frac{d}{dt} SoC(t). \quad (10)$$

The power can easily be calculated from (10).

$$P_{bat.}(t) = -\frac{U_b Q_{rated.}}{\eta} \frac{d}{dt} SoC(t). \quad (11)$$

3 Proposed control strategy of the energy storage system

3.1 Proposed Power Flow Control Method

DC microgrids receive the power from three primary types of the power sources. These power sources include the PV (photovoltaic) modules, battery packs and utility grid. The primary purpose of the power flow control is to deliver enough power to the load units. The proposed power flow control algorithm and structural diagram are given in Figure 3, and Figure 4, respectively. In the proposed algorithm, two types of switching states are assumed. When switching state is 1, the corresponding unit (PV, Battery or grid) is connected to the

load unit. When the state is 0, the corresponding unit does not supply the load. Regarding battery charging states, three states are defined; 1-charging, -1- discharging, 0-open circuit.

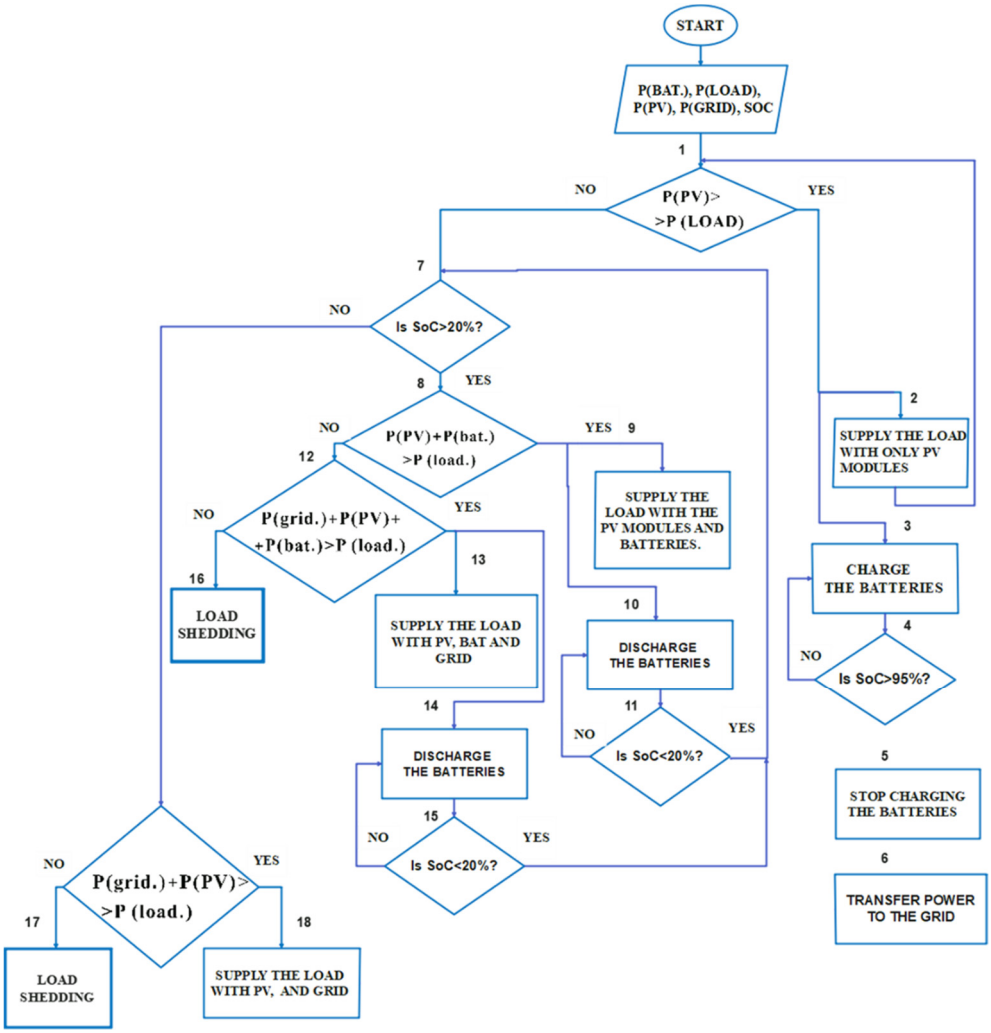

Fig. 3. The proposed flow control algorithms.

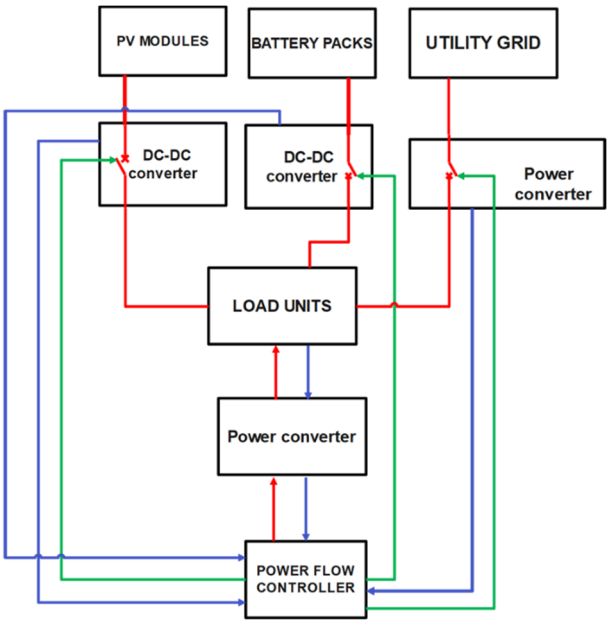

Fig. 4. Power flow control structure.

The proposed flow control employs the following procedures:

First, total power from PV units $\sum_0^N P_{PV}$, total power from battery units $\sum_0^N P_{BAT.}$, available grid power P_{GRID}, total load power $\sum_0^N P_{LOAD.}$ must be identified.

If $\sum_0^N P_{PV} > \sum_0^N P_{LOAD.}$, then PV modules are enough to supply the load with enough power without the need for battery and grid power. It is illustrated in Figure 5 where $\sum_0^N P_{PV}$ is 60W, while $\sum_0^N P_{LOAD.}$ is 40 W. The operation numbers refer to the proposed algorithm in Figure 3. In this case, battery units start charging until their SoC level is 95% to prevent overcharging. If the SoC level goes beyond the pre-defined threshold, battery units stop charging and the excessive energy is transferred to the grid. Exported energy to the grid is the following (12):

$$P_{GRID.} = \sum_0^N P_{PV.n} - \sum_0^N P_{LOAD.n}. \quad (12)$$

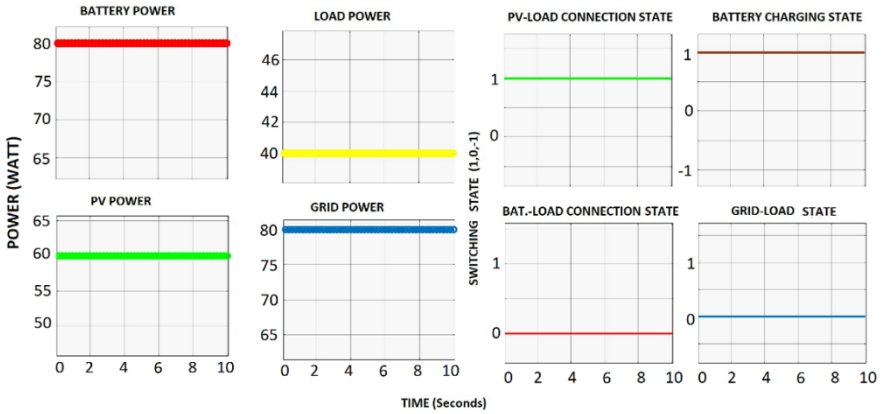

Fig. 5. The states of the switches in the proposed algorithm for the operation 2, 3.

If $\sum_0^N P_{PV} < \sum_0^N P_{LOAD.}$, then PV module output power cannot match the demand power, which necessitates the additional battery connection $\sum_0^N P_{BAT.}$. It checks the SoC level of the battery whether it is higher than 20%. If this condition is true, then the condition $\sum_0^N P_{PV} + \sum_0^N P_{bat.} > \sum_0^N P_{load}$ is checked. If it is also satisfied then batteries are connected to the load and discharging process starts (state -1) until the SoC drops to below 20% . It is illustrated in the Figure 6 where $\sum_0^N P_{PV}$ is 30W, $\sum_0^N P_{bat.}$ is 80W , SoC=75%, while $\sum_0^N P_{LOAD.}$ is 70W.

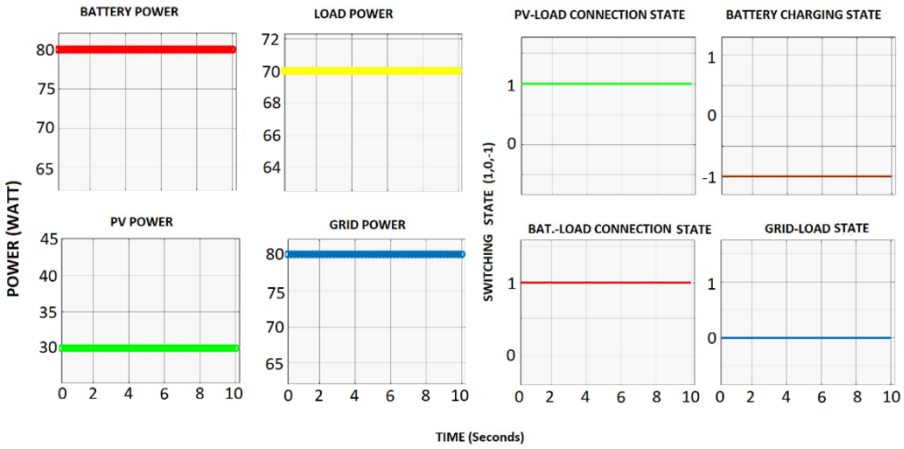

Fig. 6. The states of the switches in the proposed algorithm for the operation 9, 10.

If the battery SoC>20%, while $\sum_0^N P_{PV}$+$\sum_0^N P_{BAT.}$ cannot deliver the demand power to load, then the utility grid is switched on to be connected to the load. PV modules, batteries and the grid is connected to the load. Batteries discharge in this mode. It is illustrated in the Figure 7 where $\sum_0^N P_{PV}$ is 30W, $\sum_0^N P_{bat.}$ is 30W, SoC=75%, available $P_{GRID.} = 80$W ,while $\sum_0^N P_{LOAD.}$ is 70W. Imported energy from the grid is the following (13):

$$P_{GRID.} = \sum_0^N P_{LOAD.n} - \sum_0^N P_{PV.n} - \sum_0^N P_{bat.n}. \quad (13)$$

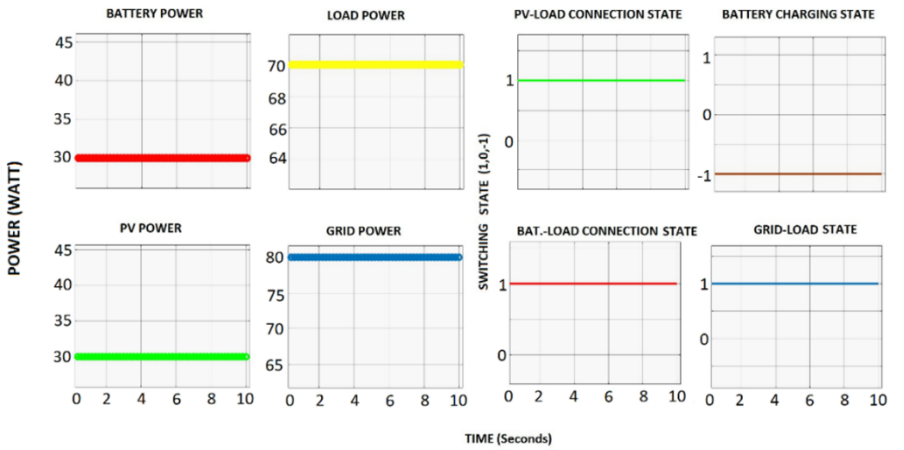

Fig. 7. The states of the switches in the proposed algorithm for the operation 13, 14.

If the battery SoC<20%, then the utility grid is switched on to be connected to the load to contribute to the PV. Batteries are disconnected in this mode because of the low SoC level.

It is illustrated in the Figure 8 where $\sum_0^N P_{PV}$ is 30W, $\sum_0^N P_{bat.}$ is 30W, available $P_{GRID.} =$ 80W ,while $\sum_0^N P_{LOAD.}$ is 70W.

Imported energy from the grid is the following (14):

$$P_{GRID.} = \sum_0^N P_{LOAD.n} - \sum_0^N P_{PV.n}. \quad (14)$$

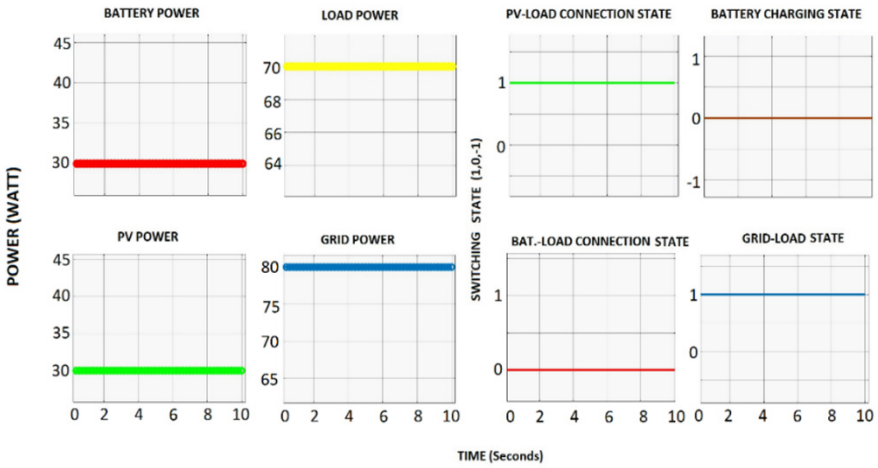

Fig. 8. The states of the switches in the proposed algorithm for the operation 18.

It is possible that the grid power is not available or not enough. Under these circumstances all power sources are switched on (unless battery SoC<20%), then the system goes to the load shedding mode, in which low priority load units are disconnected until the total power of sources can meet the demand, at least, power of high priority loads.

4 Conclusion

In conclusion, this paper highlights the importance of power flow control systems in DC microgrids with photovoltaic inputs to ensure a continuous power supply to the load. An improved power flow control method of energy sources to the load unit based on a State-of-Charge using Coulomb counting method is proposed to ensure an uninterrupted power supply. The bidirectional SEPIC-ZETA converter is chosen as an interface between the battery units and DC bus, as it allows charging and discharging of the battery units without the need for changing DC bus voltage. The proposed approach ensures that the load consistently receives the required power, and grid power is used only when the estimated combined power from the photovoltaic units and batteries is under the load demand power. A working algorithm is designed and simulations are carried out. The simulation results of the proposed approach show that it provides satisfactory control performance to meet the load demand power and can be implemented in various DC microgrid applications to enhance their performance. Overall, the proposed approach is effective in meeting load demand power and can significantly improve the performance of DC microgrid systems.

References

1. R. Kandari, N.A Mittal, Chapter 4 - DC microgrid, Microgrids, Academic Press, Pages 91-139, (2022) ISBN 9780323854634

2. M. Saad Bin Arif, M. Asif Hasan, 2 - Microgrid architecture, control, and operation, In Woodhead Publishing Series in Energy, Hybrid-Renewable Energy Systems in Microgrids, Woodhead Publishing, Pages 23-37, (2018), ISBN 9780081024935
3. S. Pannala, N. Patari, A. K. Srivastava and N. P. Padhy, "Effective Control and Management Scheme for Isolated and Grid Connected DC Microgrid," in IEEE Transactions on Industry Applications, vol. 56, no. 6, pp. 6767-6780, Nov.-Dec. (2020)
4. Z. Wang et al., "Research on the active power coordination control system for wind/photovoltaic/energy storage," IEEE Conference on Energy Internet and Energy System Integration (EI2), Beijing, China, pp. 1-5, (2017)
5. Z. Shi, W. Wang, Y. Huang, P. Li and L. Dong, "Simultaneous optimization of renewable energy and energy storage capacity with the hierarchical control," in CSEE Journal of Power and Energy Systems, vol. 8, no. 1, pp. 95-104, Jan. (2022)
6. F. O. Ramos, A. L. Pinheiro, R. N. Lima, M. M. B. Neto, W. A. S. Junior and L. G. S. Bezerra, "A Real Case Analysis of a Battery Energy Storage System for Energy Time Shift, Demand Management, and Reactive Control," IEEE PES Innovative Smart Grid Technologies Conference - Latin America (ISGT Latin America), Lima, Peru, pp. 1-5, (2021)
7. Y. R. Rodrigues, M. R. Monteiro, A. C. Zambroni de Souza, P. F. Riberiro, L. Wang and W. Eberle, "Adaptative Secondary Control for Energy Storage in Island Microgrids," IEEE Power & Energy Society General Meeting (PESGM), Portland, OR, USA, pp. 1-5, (2018)
8. J. Stuchlý and J. Vramba, "Analyses of power quality and voltage variation of photovoltaic power plant connected into 22 kV public grid," 13th International Conference on Environment and Electrical Engineering (EEEIC), Wroclaw, Poland, , pp. 48-51, (2013)
9. Z. Ben Mahmoud, M. Hamouda and A. Khedher, "Effects of series and shunt resistances on the performance of PV panel under temperature variations," International Conference on Electrical Sciences and Technologies in Maghreb (CISTEM), Marrakech & Bengrir, Morocco, pp. 1-7, (2016) doi: 10.1109/CISTEM.2016.8066772
10. B. S. Bhangu et al., “Nonlinear observers for predicting state-of-charge and state-of-health of lead-acid batteries for hybrid-electric vehicles,” IEEE transactions on vehicular technology, vol. 54, no. 3, pp. 783-794, (2005)
11. M. R. A. Ratul, "Energy Management of a Renewable Hybrid Isolated DC Microgrid," Int. J. Res. Appl. Sci. Eng. Technol., vol. 9, no. 11, pp. 116–123, Nov. (2021)
12. Z. Miao, L. Xu, V. R. Disfani, and L. Fan, "An SOC-Based Battery Management System for Microgrids," IEEE Trans. Smart Grid, vol. 5, no. 2, pp. 966–973, Mar. (2014)
13. Ma, T.T.H.; Yahoui, H.; Vu, H.G.; Siauve, N.; Morel, H. A Control Strategy of DC Building Microgrid Connected to the Neighborhood and AC Power Network. Buildings, 7, 42 (2017)
14. F. Li, Z. Lin, Z. Qian and J. Wu, "Active DC bus signaling control method for coordinating multiple energy storage devices in DC microgrid," 2017 IEEE Second International Conference on DC Microgrids (ICDCM), Nuremburg, Germany, pp. 221-226 (2017)
15. E. Yusubov and L. Bekirova, "Adaptive Metaheuristic Moth-Flame Optimized Droop Control Method for DC Microgrids," International Conference Automatics and Informatics (ICAI), Varna, Bulgaria, pp. 204-209 (2022)